Aerodynamic Design of a Axial Turbine Stage for a Small Gas Turbine Engine

S. N. Agnimitra Sunkara, Prathapanayaka Rajeevalochanam, and N. Vinod Kumar

Abstract Compact high speed turbomachines are complicated in aerodynamic design, mechanical construction, and fabrication. Design choices made during the aerodynamic design are strongly coupled to the mechanical integrity due to high rotational speeds and thermal gradients. In the present paper, aerodynamic design of a turbine with a low pressure ratio of 2:1 is presented. The turbine designed is a compact single stage machine, intended to be used in a 1 kN thrust small gas turbine engine. For the present work, the flow path is a constant hub and shroud radius rotor design, with a hub-tip ratio of 0.72. Overall guidelines used for parameter selection in velocity triangles, mean-line design and blade geometry are discussed. The turbine is designed for a mean section reaction of about 25%. Performance evaluation and flowfield analysis for the turbine geometries are carried out using a three-dimensional RANS solver. Performance characteristics of the turbine are generated for a range of pressure ratio at design speed. The intended efficiency of the turbine stage at design point is 88%. Challenges during the design process to obtain blade geometries with wide blade passage throat are put forth. The choices made in aerodynamic design which affect the ease of machining of the stator and rotor components are also brought out.

Nomenclature

C	Velocity
C_p	Specific heat at constant pressure
CFD	Computational fluid dynamics
P	Pressure [kPa]
M	Mass flow rate [kg/s]
MFF	Mass flow function $(M\sqrt{T_{01}})/(P_{01})$ [(kg/s) $\sqrt{}$K/kPa]
N	Rotational speed [rpm]

S. N. Agnimitra Sunkara · P. Rajeevalochanam (✉) · N. Vinod Kumar
Propulsion Division, CSIR-NAL, Bangalore, Karnataka, India
e-mail: prathap@nal.res.in

G. Sivaramakrishna et al. (eds.), *Proceedings of the National Aerospace Propulsion Conference*, Lecture Notes in Mechanical Engineering,
https://doi.org/10.1007/978-981-19-2378-4_10

RANS	Reynolds averaged Navier–Stokes
SF	Speed function $= N/\sqrt{(\gamma T_{01})}$ [rpm/$\sqrt{}$K]
SST	Shear stress transport
SWF	Specific work function $= (C_p \Delta T_0)/T_{01}$ [kJ/kg K]
T	Temperature [K]
Tmax	Maximum blade thickness [mm]
U	Blade speed
$y+$	Non-dimensionalized wall cell width

Subscripts

a	Axial component
m	Related to mean radius
0	Stagnation quantity
1	Turbine inlet station

Greek

η	Efficiency $= \Delta T_0/(T_{01}\ (1 - (1/\pi)^{(\gamma-1)/\gamma})$
π	Turbine total pressure ratio
φ	Flow coefficient $= C_a/U_m$
ψ	Stage loading coefficient $= (C_p \Delta T_0)/(U_m)^2$
Λ	Turbine stage reaction (pressure based)
ξ	Pressure loss coefficient $= \Delta P_0/(P_0 - P)_{\text{exit}}$

1 Introduction

Small gas turbines are a promising source of energy in power generation and UAVs. There is an ever increasing need for efficient power plants at all scales. Small gas turbines have been used as turbojets in both civilian and strategic applications [1–3]. They also have found their place in portable and micro-power generation units [4, 5]. CSIR-NAL, propulsion division has been developing small gas turbine for a 1 kN thrust UAV application. A high speed axial turbine is designed for the same. The salient parameters of the turbine are as shown in given Table 1.

With the advent of computer aided techniques, it has become easy-to-design, analyze and model almost anything with basic knowledge of a system. Recent day programs enable design software to have several discrete design modules packed into a suite. In the present work, mean-line design, blade profile generation, and 3D blade

Table 1 Turbine salient parameters

Parameter	Value
π	2.00
ψ	1.3
φ	0.66
Λ	25%
η	88%
MFF	0.1466
SWF	161.19
SF	1265.77
Hub–tip ratio	0.72
Exit flow angle	5°

stacking are carried out using a commercial turbo-machinery design suite of concepts NREC. For this purpose, a few open source turbo-machinery design software T-AXI [6], TBlade-3 [7, 8], MULTALL [9] developed by academics using legacy programming languages are also available with limited features. Turbo-machinery design and development is still seen as a very complicated affair due to the expense of money, time, and expertise, and it requires for a satisfactory design. Often times, a quick 'design-manufacture' turn-around is due to expertise gained and standardized methodology developed over a span of time. Majority of literature available on turbo-machinery design is focused only on very specific aerodynamic or mechanical aspects. But it is rare to mention about the problems or challenges faced during initial design phase where majority of choices are made. It is not unusual for designers to face a dilemma in terms of assigning weightage to aerodynamic performance, structural integrity, and manufacturing concerns. But most of the times factors like manufacturing cost, component mechanical reliability, simplicity in design, and ease in assembly outweigh the benefits of a minor aerodynamic performance increment. This work is an attempt by the authors to share their experiences in aerodynamic design with emphasis on arriving at an easy-to-manufacture design for a high speed axial turbine.

2 Aero-thermodynamic Design of Turbine

2.1 Meridional Flowpath Sizing

Turbine sizing is carried out based on meridional Mach number distribution along axial direction. For the present design, an inlet Mach number of maintained around 0.25–0.27 is maintained. Turbine nozzle exit Mach number is fixed for an average value around one. The stage outlet absolute Mach number at rotor outlet is maintained less than 0.55. The swirl angle at the turbine exit is targeted to be less than 20°. Based

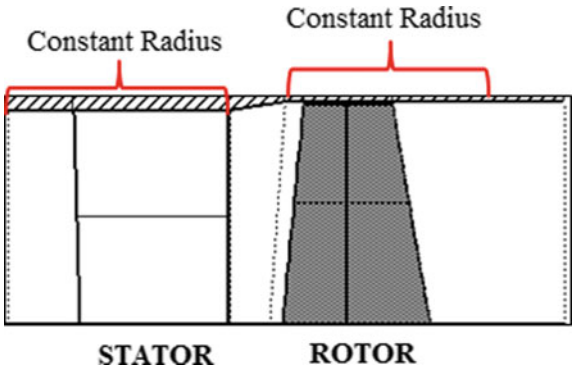

Fig. 1 Meridional flowpath

on these preliminary flowpath sizing guidelines the hub and shroud dimensions are arrived. This provides initial estimates of the flow and loading coefficients. If the flow and loading coefficients are too high or too low, the mean radius needs to be altered and checked for stress parameter AN^2, endwall flare angles, and flow swirl. A constant hub and constant shroud configuration eases the manufacturing or machining of shroud. A rotor configured to be encased within the shroud of stator reduces an extra part as shown in Fig. 1. A constant shroud allows the rotor to move axially without having to reduce the tip clearance.

2.2 Mean-Line Design

Mean-line design, velocity triangle selection is carried out by choosing the most optimum reaction level. The effectiveness of a mean reaction is not purely an aerodynamic design choice. Stage reaction influences spanwise distribution of swirl and Mach number. A lower mean reaction gives better turbine starting characteristics due to impulse to hot gas from starter cartridge. Low reaction at hub gives higher hub shock losses in nozzle but a cooler rotor hub. In addition, a low reaction at hub with low exit flow angle makes it difficult to obtain decent blade passage convergence. For the present design, a mean reaction of 25% is chosen. Velocity triangles generated from mean-line design are as shown in Fig. 2. The absolute, relative, and blade velocities are represented by '*C*', '*W*', and '*U*', respectively.

2.3 Blade Parameter Selection

After arriving at velocity triangles, the parameters required to generate blade profiles are selected. The guidelines for these have been laid by empirical loss models by Ainley and Mathieson [10], Dunham and Came [11], Kacker and Okapuu [12],

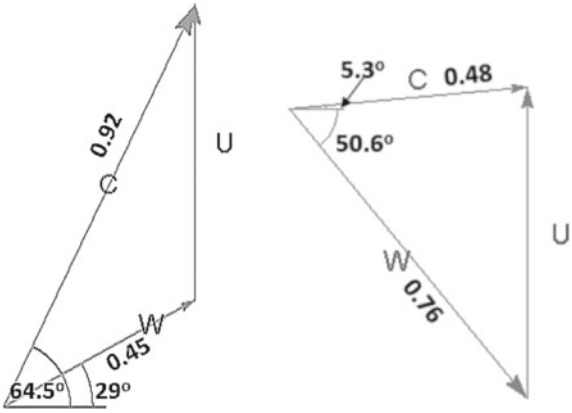

Fig. 2 Velocity triangles: mean section

(a) Rotor Inlet (b) Rotor Exit

Moustapha et al. [13] which have been in use since decades with due respect and acceptance in the turbo-machinery community. Most important primary blade parameters like blade count, chord, Tmax, and stagger are selected based on least profile loss, maximum possible passage width at the blade throat location. Stagger angle and the throat width dictate the ease with which the tool can pass through the blade passage for machining. Smaller blade passages make it difficult to achieve tight profile tolerances (through machining) which can affect the mass flow and thereby other stage performance parameters. The throat width can be estimated during this stage itself to avoid turn-around in detailed design. Most critical locations are hub throat width for both stator and rotor. It is a very good practice to consider further reduction in the throat passage at the hub/shroud locations due to introduction of fillets in final stages. If this is foreseen at the early stage, a serious shortcoming in the mass flow rate due to reduction in the flow area can be avoided. Initial estimates of blade count can also be obtained from Zweifel criterion [14] and further, looked into reducing the blade count.

Table 2 gives the choice of blade parameters used for stator and rotor mean section airfoils.

Table 2 Blade mean section parameters

Parameter	Stator	Rotor
Stagger angle	50°	30.48°
Pitch/chord	0.71	0.73
Throat/pitch	0.42	0.61
Tmax/chord	0.11	0.13
Tmax location (%C)	16.00	19.00
Aspect ratio	0.917	1.65

2.4 Blade Airfoil Design for Aerodynamic Performance and Manufacturing Ease

For the present work, blade airfoil profiles have been generated using a modified form of Pritchard [15] parametric blade generation model. The blade chord-wise thickness distribution is dictated by leading edge radius, maximum thickness, location of maximum thickness and, inlet and exit wedge angles. Unguided turning being a critical parameter which controls the flow diffusion after the blade passage throat should be kept to a minimum as it influences the surface velocity distribution and flow deviation. As a thumb rule UGT less than six degrees is recommended, but this may sometimes yield a thin profile. For flat back transonic profiles, the UGT is almost equal to exit wedge angle. It is very essential to maintain a flat unguided surface to avoid continuous acceleration till trailing edge [16]. Nevertheless, these blade profiling guidelines are not very strict and their choice of the blade shape purely depends on profile continuity and thickness distribution. The two-dimensional airfoil losses can be assessed using a blade-to-blade CFD solution. The blade profile continuity can be improved at the leading and trailing edges by ensuring smoothness at the junction points of the LE and TE circles with the pressure and suction surfaces. For the present design, elliptical blade leading edges with 2:1 ratio are used. Any discontinuity over the blade suction surface at the throat location is smoothened by conversion to Bezier curves.

Due to constrained design parameters like low reaction and constant radius hub, the airfoil design poses challenges in surface velocity distribution. High stagger configurations yield fore-loaded airfoils which can be used as long as they do not compromise overall performance [17]. The choice of stagger of rotor blades needs to be made with ease of tool reach. A reduced twist from hub to tip also simplifies the blade geometry. But there is an aerodynamic performance penalty by using constant airfoil section rotor blades.

Nevertheless, it is possible to have a constant airfoil section blade for the stator vanes without compromising the aerodynamic efficiency. This may change the design point velocity triangles obtained during variable profile design, but it can be compensated by providing a positive lean. Having constant section stator vanes allows them to be drawn or machined as singles blanks easily. Further, the inner and outer rings of the stator shroud can be machined separately reducing the cost. The rings and the blades can be joined using high temperature brazing or electron beam welding, etc. Custom made fixtures would be required to hold the rings perfectly concentric during this process.

Apart from structural considerations, blade thickness also needs to be decided based on the possible warpage or distortion withstanding machine tool loads. An easy-to-machine rotor will have tool access from the top so as to avoid several tool and work piece axis rotation operations. For a BLISK (bladed disk) rotor configuration, it is the easiest to machine a rotor blade, whose blade passages when viewed normal from the top, the pressure surface of one blade and the suction surface of neighboring blade should be visible. Blades designed with this target will have better

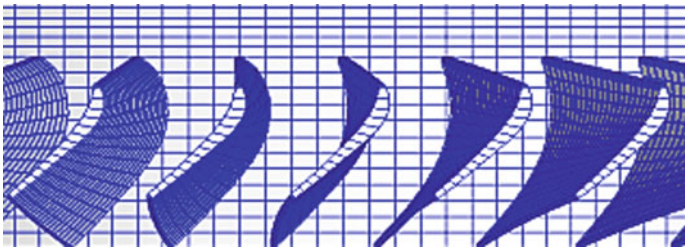

Fig. 3 Rotor blade passage

tool access and ease in machining. For moderate volume production using machining, this multiplies as a huge time saving.

Figure 3 shows the rotor blade passage whose majority of passage is accessible easily using a machining tool on a 5-axis CNC machine.

2.5 Three-Dimensional Blade Design

To obtain complete geometry, the stator airfoils are stacked about their trailing edges and the rotor blade is obtained by stacking the airfoils about their centers of gravity. Sometimes, it becomes difficult to deviate from the mean-line design dimensions owing to efficiency, reaction, swirl, and dimensional constraints. For this, a positive lean around 15–30° gives an excellent flexibility in achieving improved efficiency due to spanwise relaxation in the reaction distribution. Increase in number of geometric features increases design complexity, manufacturing time and cost. For a low cost design, choice of material needs to be solely based on availability. Simple design and reduced number of geometric features in turbine disk cross-section, seal give a significant cost reduction. Detailed design considerations in aerodynamic and thermo-structural aspects of turbine using state-of-the-art design and analysis tools are dealt in [18].

3 Numerical Set Up and Analysis

Turbine aerodynamic performance is predicted using steady RANS CFD solver ANSYS-CFX. The turbine domain is modeled as single passages of stator and rotor connected via a stage interface, through which circumferential averaging of mass, momentum, and energy fluxes is performed. A no-slip, adiabatic wall condition is applied to all the hub, shroud, and blade endwalls.

3.1 Boundary Conditions

At the domain inlet; total pressure, temperature, and swirl angle are enforced. Turbulence intensity of 8% and length scale of 1% blade height are assigned. An exit static pressure is assigned at mean radius by considering radial equilibrium. Shear stress transport (SST $k - \omega$) model [19] is used to model the RANS equation.

3.2 Grid Generation

Grid generation for the turbine domain is performed using AutoGrid5 tool of NUMECA software. O4H topology is used in generation of structured grid using hexahedral elements. Grid is generated with a near wall expansion ratio of 1.2 and minimum orthogonality of 20°. Grids are generated along with fillets ensuring excellent grid connectivity and orthogonality as shown in Figs. 4, 5, 6, 7 and 8. It is ensured that the grids used for CFD simulations yield $y+ < 11$ for SST turbulence model as per the solver requirements [20].

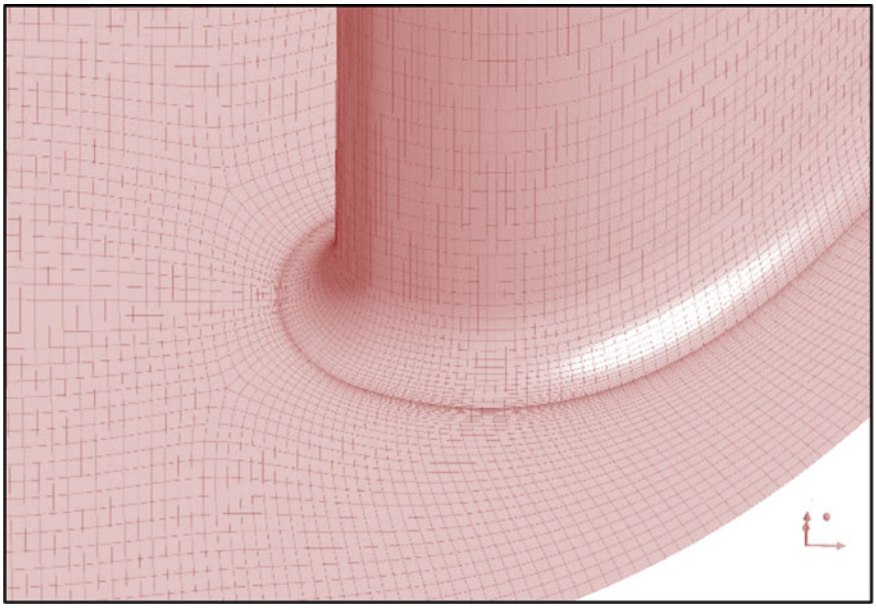

Fig. 4 Stator grid detail—leading edge

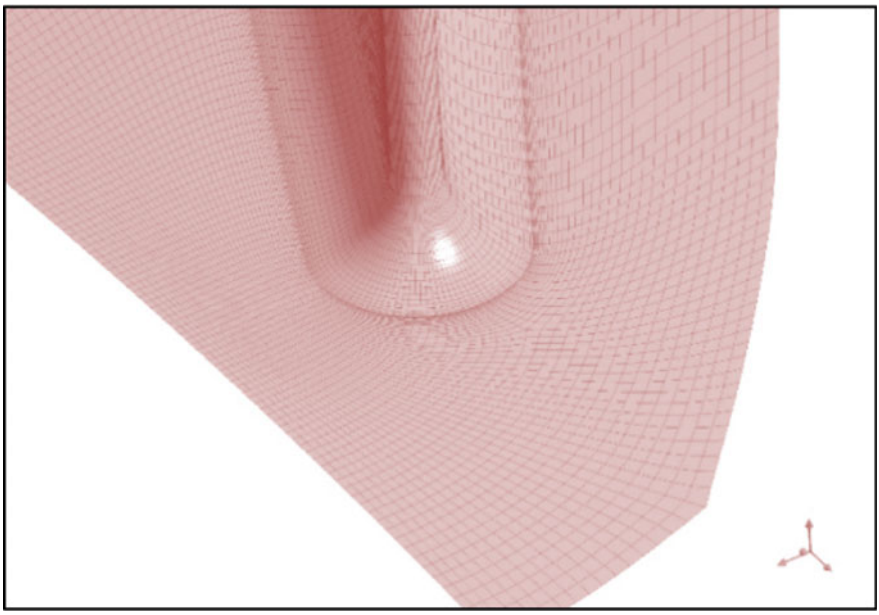

Fig. 5 Stator grid detail—trailing edge

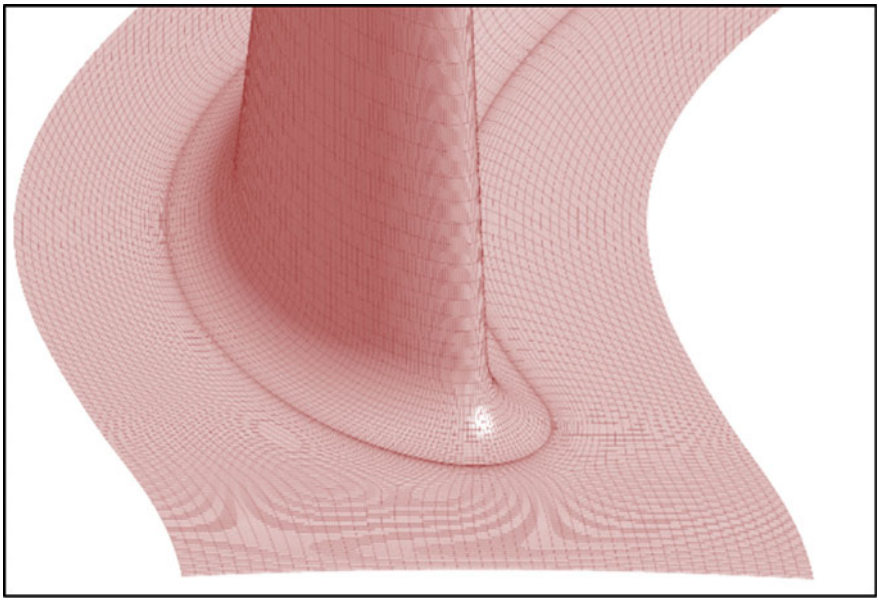

Fig. 6 Rotor grid detail—leading edge

Fig. 7 Rotor grid detail—trailing edge

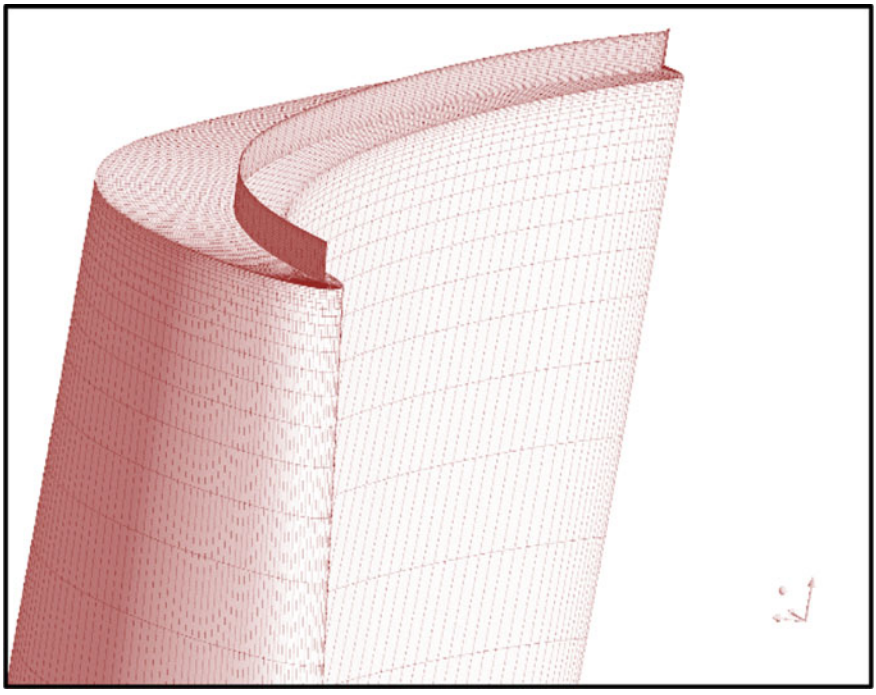

Fig. 8 Rotor tip clearance grid detail

3.3 Grid Independence Study

Size refinement is carried out, and the turbine performance is assessed. The grids are doubled successively and checked for a change in the performance variables. The criterion used is that the deviation of mass flow and the specific work should be by less than 0.2% for two consecutive meshes. From the grid dependence study as shown in Table 3, grid with size 2.7 million is chosen for further detailed analysis.

A distortion free grid is obtained for both the stator and rotor fillet endwall regions.

The tip clearance region (as shown in Fig. 8) of the size independent mesh (2.7 million) consists of about 21 grid points radially.

Figure 9 shows that the grids used for CFD simulations yield a wall $y+ < 5$. From the detailed study of grid parameters, it can be summarized that the chosen grid is sufficient to carry out detailed performance studies.

Table 3 Grid dependence study

Grid size	MFF	SWF
0.7 million	0.1466	162.93
1.3 million	0.1467	163.55
2.7 million	0.1468	163.61
5.9 million	0.1467	163.38

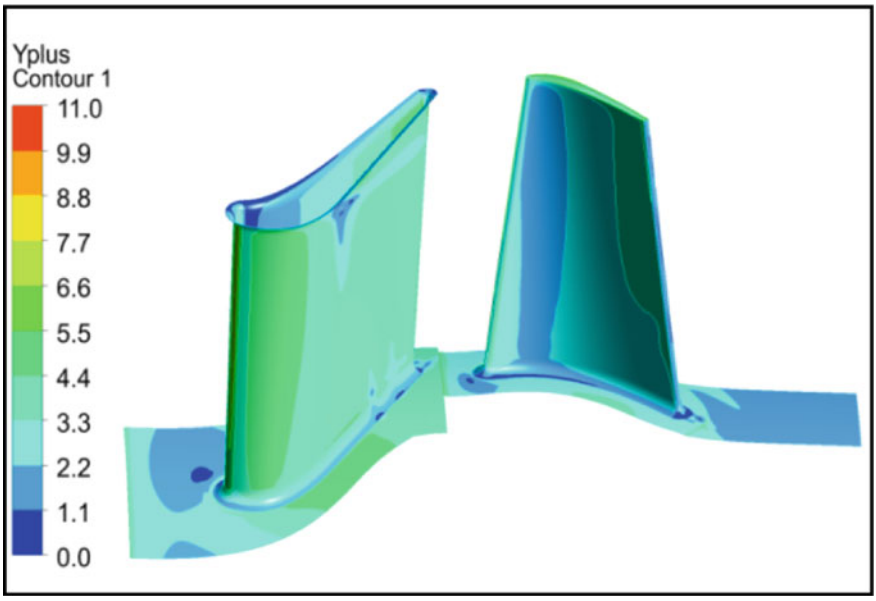

Fig. 9 Endwall $y+$ distribution

4 Turbine Performance and Flowfield Results

4.1 Turbine Performance

The aerodynamic performance of the axial turbine is assessed for a range of pressure ratio at design speed. For verification purposes, simulations are carried out for both filleted and non-filleted turbine geometries at design point and the comparative performance is shown in Table 4.

For the same exit static pressure, the presence of fillet caused a mass flow reduction of 0.3% with respect to the no-fillet case. The overall pressure ratio and specific work also changed slightly causing shift in the efficiency by 0.08%. As it is more accurate to analyze the performance considering the blade fillets as they take into consideration the actual reduction in area at the blade endwall junctions, performance of the filleted turbine geometry is assessed for a range of pressure ratio at design speed.

The turbine is clearly operating in choked region as shown in Fig. 10.

The work and efficiency characteristics in Figs. 11 and 12 show that the turbine performance is better than the design intent by approximately 1%. In addition, the turbine also exhibits a flat performance curve over a range of operating pressure ratio adjacent to the design point. This can be attributed to the incidence tolerance and thin leading edges possible through the use of elliptical leading edges.

Table 4 Aerodynamic performance

Parameter	No-fillet	Fillet
π	1.99	1.988
MFF	0.1473	0.1468
SWF	163.57	163.61
η	89.99	89.91

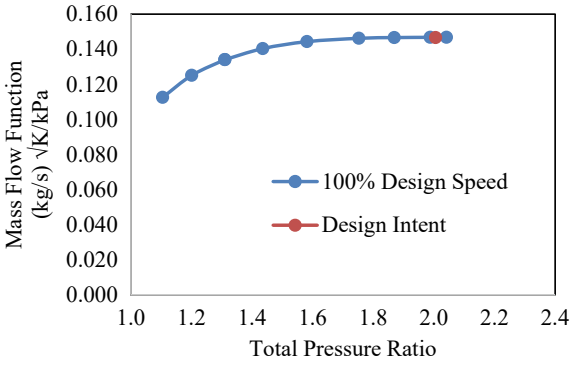

Fig. 10 Turbine mass flow characteristics

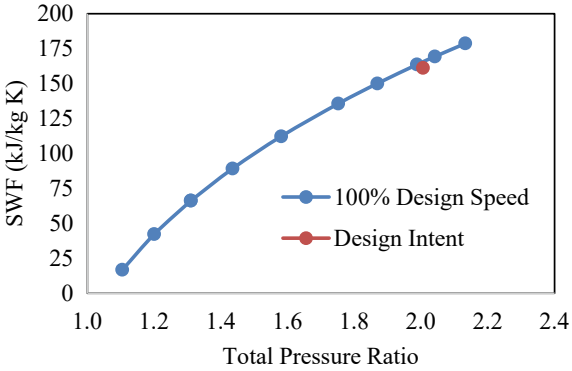

Fig. 11 Turbine work characteristics

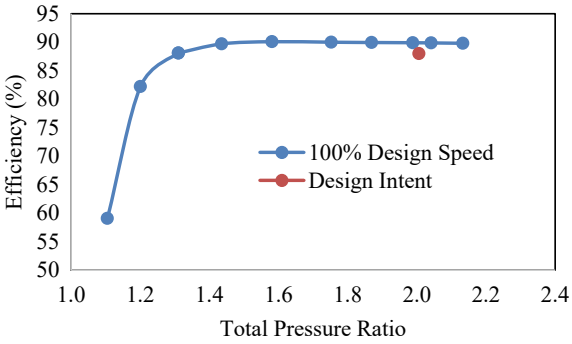

Fig. 12 Turbine efficiency characteristics

4.2 Turbine Mean Section Flowfield

Blade loading of the mean sections of stator and rotor rows is expressed as normalized surface pressure variation across blade axial chord.

For the stator vane, both the suction and pressure surfaces are free from any serious shocks as shown in Fig. 13. This can also be observed in the Mach number distribution in Fig. 15. There are no serious accelerations after the throat location around 52% of axial chord.

From the rotor blade, mean pressure loading as shown in Fig. 14 and it can be observed that the suction surface of the rotor is fore-loaded due to highly staggered rotor blades. But, there are no strong shocks on the suction surface, complemented by velocity distribution in mean section represented by Mach number contour as shown in Fig. 15. This can be owed to a combination of low stage pressure ratio and low rotor reaction.

Also, there is no significant flow deviation in stator or row rows as seen in Fig. 15.

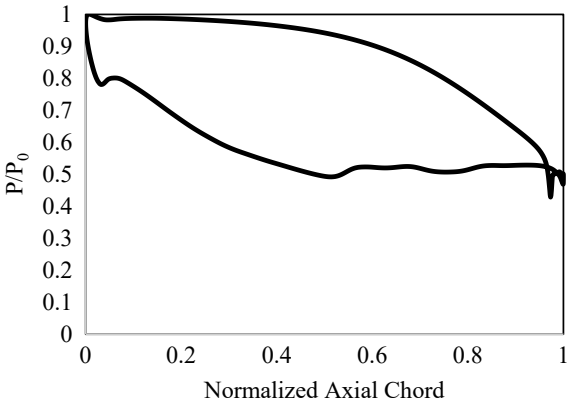

Fig. 13 Blade loading—stator vane mean section

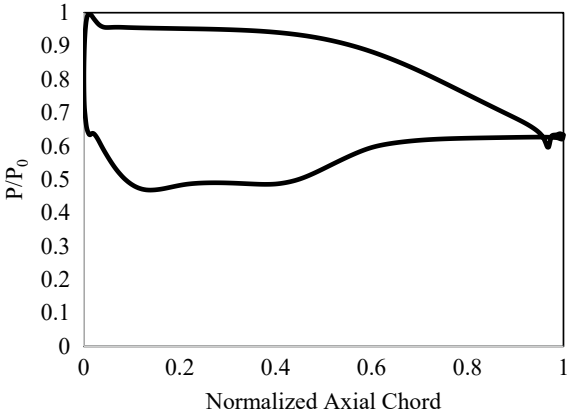

Fig. 14 Blade loading—rotor blade mean section

4.3 Turbine Spanwise Flow Analysis

The circumferentially averaged spanwise distribution of total pressure loss across stator and rotor blade rows is shown in Figs. 16 and 17.

As per the CFD result at design point, mean section loss is 4.7% and 6.9%, respectively, for stator and rotor blades. The average losses across the stator and rotor rows are 8.07% and 11.9%, respectively. From Fig. 16, it is inferred that the endwall effects in stator are well contained within 10% of blade span from both hub and shroud.

The rotor exhibits localized peak loss regions at nearly 30% and 80% of blade span, attributed to the hub passage vortex, and tip leakage vortex, respectively, as shown in Fig. 17. It can be said that from mean to nearly 70% of blade span is a vortex free zone. This is common in blades with very less annular height. The endwall flow features significantly affect the core flow. These can be mitigated using

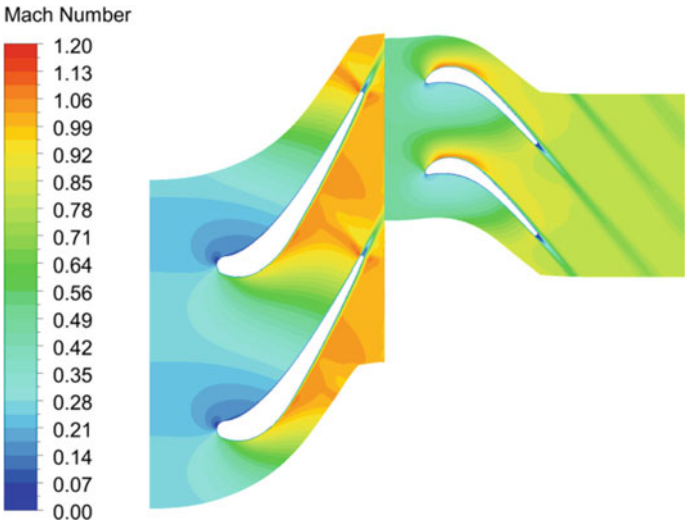

Fig. 15 Mach number distribution—mean section

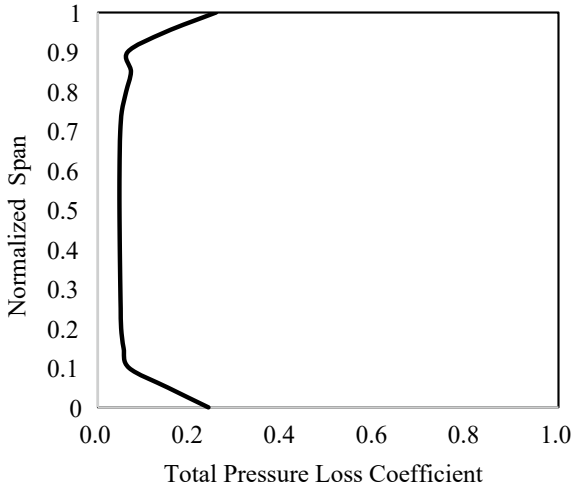

Fig. 16 Spanwise stator loss distribution

several secondary and tip clearance treatment methods. But these increase the design complexity of the turbine vanes and blades.

Figure 18 outlines that the spanwise reaction of the turbine varies linearly from hub to shroud and the mean section reaction is of 25% and is achieved as per the target. The hub reaction is maintained at 8%.

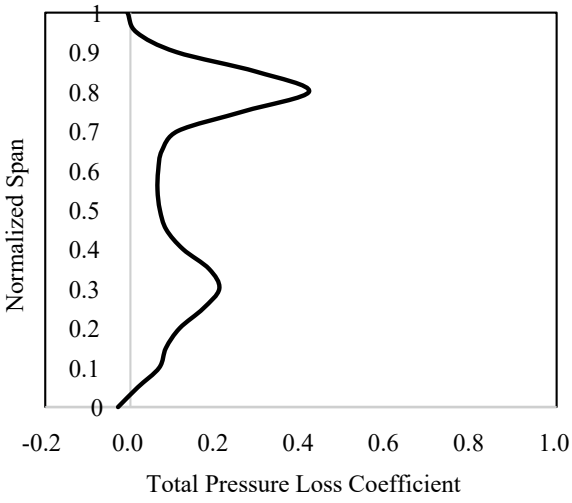

Fig. 17 Spanwise rotor loss distribution

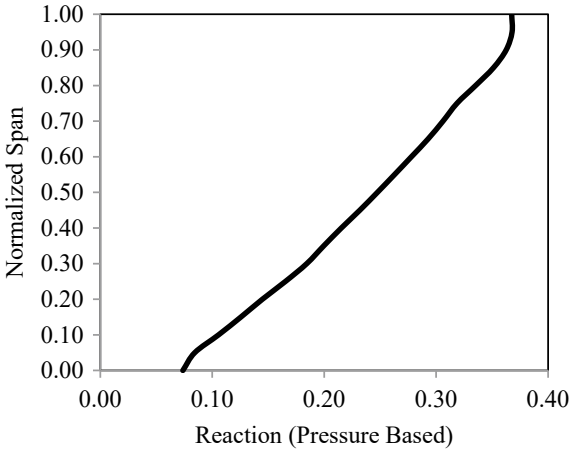

Fig. 18 Spanwise reaction distribution

5 Conclusions

A compact turbine design for a given set of salient parameters is designed, and methodology is demonstrated. The choice of basic flow path and blade parameters influencing the aerodynamic performance, and machining complexity are discussed in detail. The turbine efficiency from RANS CFD predictions is 90% against intended 88% from mean-line design. The targeted mean reaction of 25% is achieved. This is achieved due to improved aerodynamic performance of stator and rotor airfoils by incorporating elliptic leading edges, thin trailing edges, flat unguided turn, and stator positive lean. Various possibilities in simplifying the geometry for machining point of view, in terms of tool reach and reduced number of operations are put forth. Detailed

analysis over and across the turbine stator and rotor rows yields a satisfactory flow field distribution.

References

1. Jean-François R, Gilles G, Alain C, "MICROTURBO families of turbojet engine for missiles and UAV's from the TR60 to the New bypass turbojet engine generation", AIAA 2008–4590. In: 44th AIAA/ASME/SAE/ASEE Joint Propulsion Conference & Exhibit 2008
2. Razinsky E "The J402-CA-702-A modern 1000 lb thrust RPV engine". In: Proceedings of AIAA 24th Joint Propulsion Conference-1988, Paper No. AIAA-88-3248
3. Barbeau DE (1981), "A family of small, low cost turbojet engines for short life applications" In: Proceedings of ASME-Gas Turbine Conference-1981, Paper No. 81-GT-205
4. McDonald CF, Rodgers C (2002), "The ubiquitous personal turbine—a power vision for the 21st century". J Eng Gas Turbines Power 124:835–844,2002
5. De Paepe W, Carrero MM, Bram S, Parente A, Contino F (2017), "Towards higher micro gas turbine efficiency and flexibility—humidified mGTs: a review", J Eng Gas Turbines Power 140(8):081702(8),2017
6. Turner MG, Merchant A, Bruna D, University of Cincinnati T-Axi website. http://gtsl.ase.uc.edu/T-AXI/
7. Siddappaji K, Sharma M, Nemnem A, Hussain Mahmood SM, Balasubramanian K, Galbraith MC, Turner MG, University of Cincinnati T-Blade3 website. http://gtsl.ase.uc.edu/t-blade3/
8. Siddappaji K, Turner MG, Merchant A, "General capability of parametric 3D blade design tool for turbomachinery". In: Proceedings of ASME Turbo Expo 2012, GT2012-69756
9. Denton JD, "Multall-An open source, cfd based, turbomachinery design system". In: Proceedings of ASME Turbo Expo 2017, GT2017-63993
10. Ainley DG, Mathieson GCR (1951), "A method of performance estimation for axial flow turbines". British ARC, R & M 2974
11. Dunham J, Came PM (1970), "Improvements to the Ainley/Mathieson method of turbine performance prediction". ASME J Eng Power 92(3):252–256,1970
12. Kacker SC, Okapuu U (1981), "A mean line prediction method for axial flow turbine efficiency". ASME paper no. 81-GT-58,1981
13. Moustapha SH, Kacker SC, Tremblay B (1990), "An improved incidence losses prediction method for turbine airfoils". ASME J Turbomach 112(2):267–276,1990
14. Zweifel O (1945), "The spacing of turbomachine blading especially with large angular deflection, the brown Boveri review", pp 436–444,1945
15. Pritchard LJ, "An eleven parameter axial turbine airfoil geometry model". ASME paper 85-GT-219,1985
16. Rajeevalochanam P, Senthil Kumaran R, Agnimitra Sunkara SN, Kalita N, Sharath PP, "Experimental and numerical studies on a curved back transonic airfoil", V001T02A013, Paper No. GTINDIA2017-4874,2017
17. Korakianitis T (1993), "Prescribed-curvature-distribution airfoils for the preliminary geometric design of axial-turbomachinery cascades". ASME J Turbomach 115/325,1993
18. Rajeevalochanam P, Agnimitra Sunkara SN, Mayandi B, Ganesh Banda BV, Chappati VSK, Kumar K, "Design of highly loaded turbine stage for small gas turbine engine". In: Proceedings of ASME Turbo Expo 2016, GT2016-56178
19. Menter FR, Kuntz M, Langtry R (2003) Ten years of experience with SST κ-ω Turbulence model. Turbul Heat Mass Transf.,2003
20. ANSYS CFX User Manual